

# Learning Transferable Kinematic Dictionary for 3D Human Pose and Shape Reconstruction

Ze Ma,<sup>1</sup> Yifan Yao,<sup>1</sup> Pan Ji,<sup>2</sup> Chao Ma<sup>1</sup>

<sup>1</sup> Shanghai Jiao Tong University

<sup>2</sup> OPPO US Research Center

{maze1234556, yao1010fan, chaoma}@sjtu.edu.cn, peterji1990@gmail.com

## Abstract

Estimating 3D human pose and shape from a single image is highly under-constrained. To address this ambiguity, we propose a novel prior, namely kinematic dictionary, which explicitly regularizes the solution space of relative 3D rotations of human joints in the kinematic tree. Integrated with a statistical human model and a deep neural network, our method achieves end-to-end 3D reconstruction without the need of using any shape annotations during the training of neural networks. The kinematic dictionary bridges the gap between in-the-wild images and 3D datasets, and thus facilitates end-to-end training across all types of datasets. The proposed method achieves competitive results on large-scale datasets including Human3.6M, MPI-INF-3DHP, and LSP, while running in real-time given the human bounding boxes.

## Introduction

3D human body reconstruction from monocular images has attracted increasing attention in recent years due to its wide range of real-world applications. A full representation of 3D human bodies usually consists of two parts: 3D pose (*e.g.*, 3D keypoints/joints) and 3D body shape. Although great progress has been made over the years by incorporating human priors (*e.g.*, joint angle limits (Akhter and Black 2015; Bogio et al. 2016), bone length ratios (Sun et al. 2017; Zhou et al. 2017) and body symmetry (Moreno-Noguer 2017)), the typical challenges still remain, in at least two aspects: (i) there lacks an end-to-end way to make full use of human priors for 3D *shape* reconstruction; (ii) shape annotations are considerably more expensive than keypoint annotations. While shape annotations can be simulated by fitting a human model to located markers (Loper, Mahmood, and Black 2014), this is a non-trivial process and only applies to the MoCap dataset. To address these challenges, we aim to learn a kinematic dictionary, in which we distill the valuable human priors into compact knowledge, to facilitate 3D human pose and shape reconstruction under a semi-supervision manner, *i.e.*, without using shape annotations during training the neural networks.

Existing 3D pose estimation approaches (Ramakrishna, Kanade, and Sheikh 2012; Zhou et al. 2016a; Akhter and Black 2015) have made attempts to learn an over-complete dictionary of keypoint locations. With the learned pose dictionary, they recover 3D keypoints from ground-truth 2D

keypoints using Orthogonal Matching Pursuit (OMP) (Ramakrishna, Kanade, and Sheikh 2012). Despite the demonstrated promising results, linearly combining the bases of the dictionary and sparse codes results in two limitations. First, the pose dictionary is learned over keypoint locations, which has high degrees of freedom and does not encode strict anthropometric priors. Second, it lacks constraints on optimizing sparse codes, leading to undesirable recovered poses that go beyond plausible space. To address these issues, we build a dictionary on the kinematic rotations rather than keypoint locations. To the best of our knowledge, we are the first to do so. Then we constrain the learning of sparse codes so that the recovered rotation always lies in the convex hull of the bases of the dictionary. This explicitly excludes the impossible rotations during inference. To achieve this, we propose a new objective function to learn the dictionary.

Equipped with the kinematic dictionary, we further embed them into the end-to-end deep learning framework. This is much different from the previous works (Ramakrishna, Kanade, and Sheikh 2012; Zhou et al. 2016a, 2015; Wang et al. 2014; Wangni et al. 2018), which emphasizes the optimization manner to use the dictionary. Our method focuses on how to benefit from the dictionaries together with a learning framework. Specifically, we decompose the kinematic rotations into the bases and predict the sparse codes to recover the kinematic rotations via deep neural networks. We avoid iterative optimization so that our method can run in real-time. To render human shape, we integrate the kinematic dictionary with a statistical human mesh model, SMPL (Loper et al. 2015), which articulates the pose of the human by Forward Kinematics. As such, our proposed network directly outputs the human meshes. We also learn a shape dictionary to constrain the shape parameters of the SMPL model, so that the human can have the natural body type. Compared to the recent end-to-end human mesh reconstruction work (Omran et al. 2018; Pavlakos et al. 2018; Kanazawa et al. 2018, 2019), we do not use any shape annotations during the training of neural networks.

In summary, the main contributions of this work are three-fold:

- We propose to learn a novel kinematic dictionary to make full use of human priors. Our kinematic prior can be seamlessly integrated with other priors, such as a shape dictionary for SMPL, to achieve better results.

- We integrate the kinematic dictionary with a statistical human mesh model to directly output 3D human shape without requiring shape annotations for training. Our method generalizes well to data with semi-supervision.
- We extensively evaluate our method on a variety of large-scale datasets, including Human3.6M (Ionescu et al. 2014), MPI-INF-3DHP (Mehta et al. 2017a), and UP-3D (Lassner et al. 2017). The proposed method achieves competitive results in comparison with the state of the arts and runs in real-time.

## Related Work

In this section, we first discuss monocular 2D pose estimation and then review the topic of 3D pose estimation from a single image. At last, we discuss mesh-based 3D human reconstruction.

**Monocular 2D Pose Estimation.** Estimating 2D pose from monocular images has achieved much success recently. On one hand, the emergence of large-scale datasets, such as LSP (Johnson and Everingham 2010), MPII (Andriluka et al. 2014), MSCOCO (Lin et al. 2014), has greatly promoted the performance of the learning-based algorithms. With more data available, the major breakthrough emerges with deep convolutional neural networks (Toshev and Szegedy 2014; Newell, Yang, and Deng 2016; Cao et al. 2017; Wei et al. 2016). Motivated by the success in 2D pose estimation, early work on 3D pose estimation first estimates 2D keypoints and then lift them to 3D space (Martinez et al. 2017; Nie, Wei, and Zhu 2017). However, the two-stage diagram is not robust to the noisy 2D estimation and cannot be optimized end-to-end. Our method is to embed a kinematic dictionary into a deep convolutional network. Without using any intermediate representation or any shape annotations, we achieve 3D human pose and body reconstruction in an end-to-end manner.

**Monocular 3D Pose Estimation.** Early work formulates the task of 3D pose estimation from monocular images as an optimization problem equipped with the pose dictionary. Ramakrishna *et al.* (Ramakrishna, Kanade, and Sheikh 2012) learn an over-complete dictionary to model the distribution of 3D pose, then optimize sparse codes to fit the recovered 3D pose projection to the observed 2D keypoints. This method motivates Zhou *et al.* (Zhou et al. 2015, 2016b) and Wang *et al.* (Wang et al. 2014) to develop better optimization algorithms. Akhter *et al.* (Akhter and Black 2015) takes one step further to use conditioned joint angle priors in an optimization way to penalize the unreasonable poses. Despite the demonstrated success, optimization does not fully utilize the valuable pose priors and image clues. With the emergence of deep learning, considerable efforts have been made to deal with 3D pose estimation by learning deep regression networks (Chen and Ramanan 2017; Martinez et al. 2017; Moreno-Noguer 2017; Nie, Wei, and Zhu 2017). These methods typically estimate 2D keypoints first and then lift them to 3D keypoints. As mentioned above, these two-stage approaches are not robust to noisy 2D keypoints

estimation and cannot be optimized end-to-end. So there comes recent work to directly estimate 3D pose from 2D images (Rogez and Schmid 2016; Sun et al. 2017, 2018; Luvizon, Picard, and Tabia 2018). These works aim to bridge this gap to facilitate end-to-end training across 2D and 3D datasets. Among them, Zhou *et al.* (Zhou et al. 2016a) manages to regress in the kinematic rotation space from monocular images and manually designs the rotation limits. On the contrary, we use a data-driven way to distill the kinematic knowledge from the MoCap dataset and then show they are also applicable in other datasets.

**3D Human Reconstruction in Mesh.** Human shape and pose reconstruction can be also viewed as an optimization problem. The pioneer methods (Bogo et al. 2016; Lassner et al. 2017) use 2D keypoints, which are generated by off-the-shelf 2D pose estimators, to fit the SMPL model. The learning-based methods directly regress SMPL parameters under different supervisions, such as vertices (Kolotouros, Pavlakos, and Daniilidis 2019), voxels (Varol et al. 2018), and 3D keypoints (Kanazawa et al. 2018). On the other hand, the input representation, such as monocular RGB images (Kanazawa et al. 2018; Tan, Budvytis, and Cipolla 2018), segmentations (Omran et al. 2018), as well as heatmaps and silhouettes (Pavlakos et al. 2018) can be fed into the network. Recently, distinguished breakthrough has been made in this area to utilize Graph Convolution (Kolotouros, Pavlakos, and Daniilidis 2019), to synergize using dense annotation (Guler and Kokkinos 2019) or to integrate SMPLify with the regression model (Kolotouros et al. 2019). Kolotouros *et al.* (Kolotouros, Pavlakos, and Daniilidis 2019) manages to directly regress vertices from single-view images. Guler *et al.* (Guler and Kokkinos 2019) uses the dense annotations in DensePose (Güler, Neverova, and Kokkinos 2018) to synergize with the SMPL. Kolotouros *et al.* (Kolotouros et al. 2019) combines the regression model (Kanazawa et al. 2018) with SMPLify (Bogo et al. 2016) to benefit from both the optimization manner and the learning manner. Dong *et al.* (Dong et al. 2020) asynchronous multi-view as a source to alleviate ill-posed issue. Although these works have demonstrated promising results, they perform regression in the SMPL parameter space without any constraints. They thus need additional supervision on SMPL parameters or using the adversarial learning to regularize the solution space. And without any supervision on the SMPL parameters, it will be hard for networks to converge or to regress natural human meshes. We notice that only a very few datasets (Ionescu et al. 2014; Akhter and Black 2015) provide such supervision signals, *i.e.*, collecting data based on markers in the controlled environment. These datasets only have a single person and simple background contexts with a large domain gap from the real data. The recent 3D pose datasets (Saini et al. 2019; Joo et al. 2015, 2017; Mehta et al. 2017a) collect in-the-wild data without markers, resulting in semi supervisions. Hence it is of great importance to utilize the possible priors to constrain the kinematic solution space. Our learned dictionary well compresses the shape annotations from the MoCap data

and can readily transfer to in-the-wild datasets. They greatly reduce the hidden solution of the kinematic rotation space and the shape space of SMPL as well. This not only accelerates the network convergence but also improves the results.

## Technical Approach

In this section, we first briefly review the SMPL model. Then we show the overview of our proposed model. After that, we carefully discuss how we learn the kinematic dictionary from data. We embed the learned dictionaries into the deep learning framework under semi-supervision. We use the dictionary to constrain the kinematic rotations in a plausible space.

### Revisiting SMPL

We use the SMPL model for its simplicity and flexibility. The SMPL model (Loper et al. 2015) provides a function  $\mathbf{M} = M(\Theta, \beta)$ , which takes as input the pose parameters  $\Theta$  and shape parameters  $\beta$ , and returns the body mesh  $\mathbf{M} \in \mathbb{R}^{3 \times P}$ , with  $P = 6890$  vertices. The pose  $\Theta \in \mathbb{R}^{4 \times K}$  is represented by the 3D relative rotations of  $K = 23$  joints in the human kinematic tree. The shape  $\beta \in \mathbb{R}^{10}$  is modeled by the first 10 coefficients of PCA in a collected shape space. The SMPL function  $M(\Theta, \beta)$  first adjusts the template shape conditioned on  $\Theta$  and  $\beta$ , and then articulates the joints via Forward Kinematics. Note that this function is fully differentiable. It also provides a pre-defined matrix  $\mathbf{Z}$  to get 3D keypoints from the mesh via linear transformation, *i.e.*,

$$\mathbf{X}_{3D} \in \mathbb{R}^{3 \times K} = \mathbf{Z}M(\Theta, \beta). \quad (1)$$

We assume a weak perspective camera model as the previous work (Kanazawa et al. 2018) so that our goal is to solve for a global rotation  $\mathbf{R}$ , a scaling factor  $s$  and a 2D translation vector  $\mathbf{t}$ , with which the 3D keypoints can be projected onto the image plane via

$$\mathbf{X}_{2D} \in \mathbb{R}^{2 \times K} = s\Pi(\mathbf{R}\mathbf{X}_{3D}) + \mathbf{t}, \quad (2)$$

where  $\Pi$  is an orthographic projection.

### Reconstructing Human Mesh via Kinematic Dictionary

Our goal is to reconstruct the 3D human mesh from a single RGB image in the form of the SMPL model, which consists of a set of parameters  $\{\Theta, \beta, \mathbf{R}, s, \mathbf{t}\}$ . We resort to a data-driven method to solve this problem with the aid of a deep neural network and our proposed kinematic dictionary.

**Overall Idea.** In the SMPL model, the pose  $\Theta$  dominates human visualization. Therefore, regularizing the pose parameters is of utmost importance for human mesh reconstruction. To this end, we propose a simple kinematic dictionary prior to encode the space of all the plausible relative rotations of 3D human joints. For each human joint, the model leverages a sparsemax layer (Olshausen and Field 1997) to predict the non-negative sparse codes  $\gamma$ , whose  $L_1$  norm equal to 1. The kinematic rotation  $\theta \in \mathbb{R}^4$  of each

joint in the quaternion representation is then recovered by a sparse linear combination of the bases in the kinematic dictionary. By doing so,  $\theta$  is forced to lie in the convex hull of bases in the dictionary. We also extend our dictionary learning method readily to build a shape dictionary for  $\beta$  to restrict the shape parameters of SMPL. We use the same camera setting as previous works (Kanazawa et al. 2018; Kolotouros, Pavlakos, and Daniilidis 2019; Omran et al. 2018) in Equation (2). The only difference is that we use the representation proposed by Zhou *et al.* (Zhou et al. 2019) for the global rotation, represented by the first two columns of the rotation matrix.

In the following sections, we elaborate on the important modifications we make to sparse coding to adapt for learning kinematic rotation, and further extend it to the shape dictionary. We would like to point out that even though the shape dictionary is SMPL-dependent, the kinematic dictionary is model-agnostic and can be utilized in other shape models (Pavlakos et al. 2019; Anguelov et al. 2005; Romero, Tzionas, and Black 2017) that share a similar kinematic tree with SMPL.

Figure 1 shows the overall pipeline of our proposed model, which can be trained in an end-to-end manner. In short, our network consists of a ResNet-50 backbone with a shared MLP to predict the pose codes, the shape codes, and the global camera parameters.

**Kinematic Dictionary.** As discussed above, in the heart of our method lies the construction of a kinematic dictionary which contains plausible 3D rotations. However, a dictionary of rotations also causes difficulties in pose reconstruction. It’s well known that the 3D rotations lie on a nonlinear  $SO(3)$  manifold, and a Linear Interpolation (Lerp) of them may lead to invalid composition (Carfora 2007). As such, a Spherical Linear Interpolation (Slerp) (Shoemake 1985) is often demanded, which hinders the use of our kinematic dictionary in the end-to-end framework. Fortunately, we observe that the relative 3D rotations of human joints only span a small subspace of the complete  $SO(3)$  manifold, which permits an approximate solution.

**From Slerp to Lerp via Sparsemax.** Considering two valid rotation quaternions  $\mathbf{q}_1, \mathbf{q}_2 \in \mathbb{R}^4$  in the dictionary, a new quaternion  $\mathbf{q}$  could be reconstructed by,

$$\begin{aligned} \mathbf{q} &= \text{Slerp}(x_1, x_2; \mathbf{q}_1, \mathbf{q}_2) \\ &= \frac{\sin(x_1\delta)}{\sin(\delta)} \mathbf{q}_1 + \frac{\sin(x_2\delta)}{\sin(\delta)} \mathbf{q}_2 \end{aligned} \quad (3)$$

s.t.  $x_1 + x_2 = 1$ ,  $x_1, x_2 \in [0, 1]$ ,

where  $\delta$  is the angle subtended by the arc from  $\mathbf{q}_1$  to  $\mathbf{q}_2$ . In the limit as  $\delta \rightarrow 0$ , which means  $\mathbf{q}_1$  and  $\mathbf{q}_2$  are close enough, Slerp can be well approximated by Lerp, *i.e.*,  $\mathbf{q} = x_1\mathbf{q}_1 + x_2\mathbf{q}_2$ . We further encourage a valid rotation recovery from Lerp by enforcing the dictionary codes to be sparse. We achieve this by the use of the sparsemax function (Martins and Astudillo 2016),

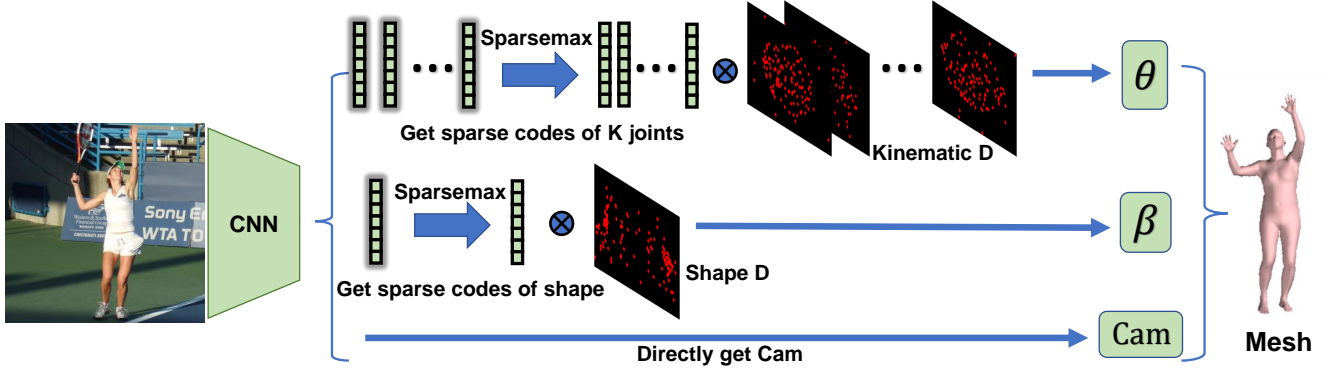


Figure 1: **Overview of the proposed model.** The network predicts the sparse codes with the help of the sparsemax layer. Afterwards, it combines the sparse codes linearly with the pre-learned kinematic dictionary and the shape dictionary to recover the valid human joint kinematic rotations and shape parameters. With the directly regressed camera parameters, we finally use the SMPL model to reconstruct the 3D human mesh.

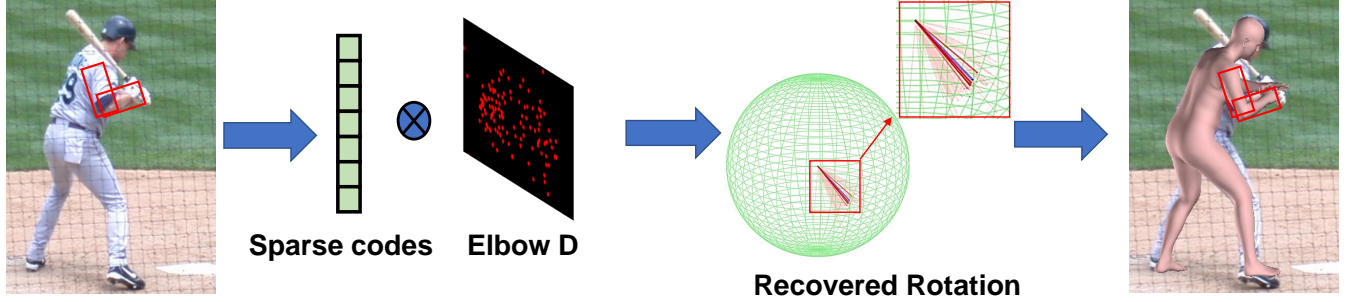


Figure 2: Visualization of how to utilize the elbow joint dictionary to get the elbow rotation. The selected atoms in the dictionary are plotted in red and the inactive ones are in transparent red. The recovered rotation is in blue. We can see that, 1) the joint rotation is constrained to a small subspace of the whole rotation space, and 2) the selected atoms in the dictionary are close enough in favor of approximating Slerp by Lerp.

$$\text{sparsemax}(z) := \underset{p \in \Delta^{K-1}}{\operatorname{argmin}} \|p - z\|^2 \quad (4)$$

where  $\Delta^{K-1} := \{p \in \mathbb{R}^K | \mathbf{1}^\top p = 1, p \geq 0\}$  is the  $(K - 1)$ -dimensional simplex. This function returns the Euclidean projection of the input vector  $z$ , which hits the boundary of the simplex, and then gets sparse output. With the distinctive feature of returning sparse posterior distributions, it can be used to identify which variables can contribute to the decision, making the model more interpretable.

We visualize the quaternions selected by sparse codes in Figure 2, which empirically validates the effectiveness of the Slerp for our kinematic dictionary. It shows that the model learns to predict sparse codes that select closer quaternions to recover the target rotation.

**Training Loss.** During the training process, our loss function is,

$$L = L_{3D} + L_{2D}, \quad (5)$$

where each term is defined as

$$\begin{aligned} L_{3D} &= \|\mathbf{X}_{3D} - \hat{\mathbf{X}}_{3D}\|_2^2, \\ L_{2D} &= \|\mathbf{X}_{2D} - \hat{\mathbf{X}}_{2D}\|_2^2. \end{aligned} \quad (6)$$

Here we reuse the terms of  $\mathbf{X}_{2D}$  and  $\mathbf{X}_{3D}$  to represent 2D and 3D keypoints. We use  $\hat{\mathbf{X}}_{3D}$  and  $\hat{\mathbf{X}}_{2D}$ , to refer to annotations.  $L_{2D}$  captures the observation of 2D keypoints and  $L_{3D}$  can help to recover depth ambiguity. Usually, these two losses are enough for the task of regressing 3D keypoint (Pavlakos et al. 2017; Zhao et al. 2019; Chen and Ramanan 2017; Martinez et al. 2017; Moreno-Noguer 2017; Nie, Wei, and Zhu 2017), but for shape recovery, models will fail without shape supervisions (Kanazawa et al. 2018). This is because human shape has much more degrees of freedom than human keypoints, so by only constraining the keypoints to be accurate, there are still different ways to fit the human model, though most of the solutions will result in unnatural visualization.

To address this, previous methods (Omran et al. 2018; Pavlakos et al. 2018) introduce shape loss on the MoCap dataset where shape annotations are available. They put su-

pervisions on SMPL parameters  $\beta$  and  $\Theta$  or on Meshes  $\mathbf{M}$ . However, it becomes inapplicable when training on in-the-wild datasets because these annotations are no longer available. In our work, we avoid training neural networks with such supervision. Instead, we distill the kinematic and shape knowledge into our kinematic and shape dictionaries, and embed these dictionaries into the deep learning network as a sparse coding layer to constrain the solution space. We show that it not only works on the MoCap dataset, from which we distill the shape knowledge, but works on in-the-wild datasets as well, which demonstrates the knowledge encoded in the dictionaries is transferable.

### Learning Kinematic Prior via Online Batch Dictionary Learning

We now show how to learn a kinematic dictionary using the prior from data. We follow the online dictionary learning work (Mairal et al. 2009) from the sparse coding community for scalable learning, but make important changes to accommodate the fact that our kinematic dictionary contains rotations as its bases. Specifically, we aim to solve an optimization problem as follows

$$\begin{aligned} \min_{\mathbf{D}, \mathbf{w}} \quad & \frac{1}{2} \|\boldsymbol{\theta} - \mathbf{D}\mathbf{w}\|_2^2, \\ \text{s.t.} \quad & \|\mathbf{w}\|_1 = 1, \mathbf{D} = [\mathbf{d}_1 \ \mathbf{d}_2 \ \cdots \ \mathbf{d}_N], \\ & \|\mathbf{d}_i\|_2^2 = 1, \forall i = 1, \dots, N. \end{aligned} \quad (7)$$

In (Mairal et al. 2009), the sparsity of  $\mathbf{w}$  is achieved by minimizing the  $L_1$  norm of  $\mathbf{w}$ . However, since here we adopt the convex combination, which requires its norm to be 1, so we propose to use the sparsemax function (Martins and Astudillo 2016) in lieu of the  $L_1$  norm, giving rise to a *smooth* objective, *i.e.*,

$$L(\mathbf{w}, \mathbf{D}) = \frac{1}{2} \|\boldsymbol{\theta} - \mathbf{D}f(\mathbf{w})\|_2^2, \quad (8)$$

where  $f(\cdot)$  represents the smooth and convex sparsemax function.

To permit fast computation, we further propose the On-line Batch Dictionary Learning (**OBDL**) that accepts data batches for data parallelism on GPUs. The learning objective becomes

$$L(\mathbf{W}, \mathbf{D}) = \frac{1}{2} \|\bar{\boldsymbol{\theta}} - \mathbf{D}f(\mathbf{W})\|_2^2, \quad (9)$$

where  $\bar{\boldsymbol{\theta}} \in \mathbb{R}^{4 \times b}$  contains a batch of quaternions with the batch size  $b$ , and  $\mathbf{D} \in \mathbb{R}^{4 \times N}$  is the quaternion dictionary to be learned with  $N$  atoms. The sparse code  $\boldsymbol{\Gamma} = f(\mathbf{W}) \in \mathbb{R}^{N \times b} = [\boldsymbol{\gamma}_1 \ \boldsymbol{\gamma}_2 \ \cdots \ \boldsymbol{\gamma}_b]$  has the sparsemax normalized columns, each of which corresponds to one sample in the batch.

Following Mairal *et al.* (Mairal et al. 2009), we adopt an alternating strategy to minimize  $L(\mathbf{W}, \mathbf{D})$ , *i.e.*, optimizing over one of the variables while fixing the other. We initialize the code  $\mathbf{W}$  from the standard Gaussian distribution, which turns out to be a good initialization for the convergence. Note that  $\mathbf{W}$  itself doesn't need to be sparse as the sparsity is guaranteed by the sparsemax  $f(\cdot)$ . As in (Mairal

---

### Algorithm 1 Learning Kinematic Prior via OBDL

---

**Require:**  $\bar{\boldsymbol{\theta}} \in \mathbb{R}^{4 \times b}$ , time step  $T$ , momentum  $\eta \in [0, 1)$ .  
1: Randomly initialize  $\mathbf{D}_0 \in \mathbb{R}^{4 \times N}$  from Gaussian.  
Reset the history information:  $\mathbf{A}_0 = \mathbf{I}_N, \mathbf{B}_0 = \mathbf{D}_0$ .  
2: **for**  $t = 1$  to  $T$  **do**  
3: Draw  $\bar{\boldsymbol{\theta}}$  from the training data, randomly initialize  $\mathbf{W} \in \mathbb{R}^{N \times b}$  from Gaussian.  
4: Update  $\mathbf{W}$  via gradient descent to minimize the objective function in Eq. (9).  
5:  $\mathbf{A}_t = \eta \mathbf{A}_{t-1} + (1 - \eta) \sum_{k=1}^b \boldsymbol{\gamma}_k \boldsymbol{\gamma}_k^T$ .  
6:  $\mathbf{B}_t = \eta \mathbf{B}_{t-1} + (1 - \eta) \sum_{k=1}^b \bar{\boldsymbol{\theta}}_t[:, k] \boldsymbol{\gamma}_k^T$ .  
7: Update  $\mathbf{D}_t$  using Algorithm 2 via block decent, with  $\mathbf{D}_{t-1}$  as warm restart, to minimize Eq. (9).  
8: **end for**  
9: **Return**  $\mathbf{D}_T$  (learned kinematic dictionary)

---



---

### Algorithm 2 Quaternion Dictionary Update

---

**Require:**  $\mathbf{D}_{t-1}$  (input dictionary),  $\mathbf{A}_t, \mathbf{B}_t$   
1:  $\mathbf{D}_t \leftarrow \mathbf{D}_{t-1}$  (initialize with a warm restart)  
2: **for**  $j = 1$  to  $N$  **do**  
3: Update the  $j$ -th column to optimize Eq. (9)  

$$\mathbf{u}_j \leftarrow \frac{1}{\mathbf{A}[j, j]} (\mathbf{b}_j - \mathbf{D}_t \mathbf{a}_j) + \mathbf{d}_j.$$
  
4: Normalize  $\mathbf{u}_j$  to get a valid unit quaternion  $\mathbf{d}_j$ ,  

$$\mathbf{d}_j \leftarrow \frac{1}{\|\mathbf{u}_j\|_2} \mathbf{u}_j, \mathbf{D}_t[:, j] = \mathbf{d}_j.$$
  
5: **end for**  
6: **Return**  $\mathbf{D}_t$  (updated dictionary)

---

et al. 2009), we use matrices  $\mathbf{A}$  and  $\mathbf{B}$  to store the history information and  $\eta$  to control the momentum. In the step of optimizing the dictionary  $\mathbf{D}$ , we normalize its columns to keep the bases valid. Overall, the optimization problem for minimizing  $L(\mathbf{W}, \mathbf{D})$  is non-convex; however, we empirically observe that the proposed alternating method converges fast with good local solutions. We summarize our dictionary learning method in Algorithm 1 and Algorithm 2.

## Experiments

This section presents the experimental validation of our method. We first overview the implementation details. Then we report the overall performance on large-scale datasets as well as the qualitative results. Last, we present ablation studies.

### Implementation Details

For dictionary learning, we learn a kinematic dictionary for each joint of the kinematic tree using in the SMPL model, resulting in a total of 23 dictionaries. We set the dictionary size to 128, and the batch size to 512. We also learn a shape dic-

tionary for shape parameters for SMPL using MoCap data in the same way.

To construct the neural network, we use Resnet-50 (He et al. 2016) as the encoder as in (Kanazawa et al. 2018; Omran et al. 2018). For each input image, we take the 2048-D convolutional features before GAP (Global Average Pooling), then pass them into an MLP consisting of two 4096-neuron fully-connected layers and a leaky-relu layer. The MLP outputs the camera parameters and the initial codes of  $\theta$  and  $\beta$ . We feed the initial codes of  $\theta$  and  $\beta$  to the sparse-max layer in the neural network to obtain sparse codes. With corresponding dictionaries, we recover  $\theta$  and  $\beta$  from their sparse codes and use SMPL to render the human mesh.

During training, we use the 3D datasets of Human3.6M (Ionescu et al. 2014), MPI-INF-3DHP (Mehta et al. 2017a), and UP-3D (Lassner et al. 2017) and in-the-wild 2D datasets of LSP, LSP-extended (Johnson and Everingham 2010), MPII (Andriluka et al. 2014) and COCO (Lin et al. 2014), as in work (Kanazawa et al. 2018). We follow previous work to train a generic model using all training data, and evaluate on each dataset respectively. Note that although we use the MoCap dataset of Human3.6M, we do not use any of its shape annotations, which can be seen from the loss function.

More details are included in the supplementary material.

## Overall Performance

Since our proposed dictionary learning scheme does not explicitly model human mesh with additional expert knowledge, *e.g.*, post-processing (Kolotouros et al. 2019), temporal clues (Kanazawa et al. 2019) or dense keypoints (Guler and Kokkinos 2019), we fairly compare with the state-of-the-art methods built directly upon the SMPL model. To evaluate the transferability of the proposed dictionary, we report the scores on a variety of datasets that do not have shape annotations. However, since most of the previous methods report results in the large MoCap dataset Human3.6M, for a fair comparison, we incorporate Human3.6M into training data but use only keypoint annotations, excluding the shape annotations provided by Mosh (Loper, Mahmood, and Black 2014).

**Human3.6M.** This large indoor MoCap dataset includes subjects performing different activities such as discussing, walking, and eating. By ruling out the shape annotations provided by Mosh, we only use keypoint annotations to supervise our model. We use subjects S1, S5, S6, S7, and S8 for training, and we evaluate on S9 and S11 following the standard protocols, P1 and P2. P1 uses S9 and S11 with all camera views as the test set and reports mean per joint position error (MPJPE) without Procrustes Alignment. P2 uses only frontal camera views of S9 and S11 and reports reconstruction error after Procrustes Alignment. Table 1 shows that our method performs well against the state-of-the-arts.

**MPI-INF-3DHP.** This dataset is collected in a markerless system with a multi-view setup. Table 2 shows that our

Method	P2↓	P1↓
Akhter <i>et al.</i> (Akhter and Black 2015)	181.1	-
Ramakrishna <i>et al.</i> (Ramakrishna, Kanade, and Sheikh 2012)	157.3	-
Zhou <i>et al.</i> (Zhou et al. 2015)	106.7	-
SMPLify (Bogo et al. 2016)	82.3	-
SMPLify from 91 kps (Lassner et al. 2017)	80.7	-
Pavlakos <i>et al.</i> (Pavlakos et al. 2018)	75.9	-
NBF (Omran et al. 2018)	59.9	-
HMR (Kanazawa et al. 2018)	56.8	88.0
Kolotouros <i>et al.</i> (Kolotouros, Pavlakos, and Daniilidis 2019)	50.1	74.7
Ours (Semi)	<b>48.6</b>	<b>66.6</b>

Table 1: Human3.6M results. The top 3 methods utilize a pose dictionary in the optimization manner and the others directly regress to SMPL parameters. We achieve competitive results in comparison with the state of the arts.

Method	After Rigid Alignment			Absolute		
	PCK↑	AUC↑	MPJPE↓	PCK↑	AUC↑	MPJPE↓
Mehta <i>et al.</i> (Mehta et al. 2017a)	-	-	-	75.7	39.9	<b>117.6</b>
VNect (Mehta et al. 2017b)	83.9	47.3	98.0	<b>76.6</b>	<b>40.4</b>	124.7
HMR (Kanazawa et al. 2018)	86.3	47.8	89.8	72.9	36.5	124.2
Ours (Semi)	<b>91.7</b>	<b>53.1</b>	<b>75.2</b>	74.2	35.2	119.5

Table 2: MPI results. Our method performs better than HMR which utilizes GAN by a large margin after rigid alignment, and is comparable without alignment.

method performs the best after alignment because the kinematic dictionary can well constrain human keypoints. Before rigid alignment, our method is comparable with HMR (Kanazawa et al. 2018) because we use the same camera setting, which yields large global rotation and translation inconsistency.

**UP-3D.** This dataset (Bogo et al. 2016) contains in-the-wild 2D images and also uses fitted SMPL parameters for evaluation. We report the results on the test set in Table 3.

**LSP.** We evaluate our method on the human body segmentation task. We do not use any segmentation labels in training. Table 4 shows the segmentation accuracy and average F1 scores both on parts and binary segmentation. Our method is on par with SMPLify, which uses ground truth keypoints and segmentation as supervision. Our method performs better than HMR in part segmentation because of the kinematic and shape dictionary are more stable than training with adversarial learning. Our method runs in real-time, much faster than other methods.

## Qualitative Results

Figure 3 includes qualitative results of our approach from different datasets involved in our evaluation, and we get excellent reconstruction even on some difficult gestures.

## Ablation Studies

We evaluate the effectiveness of dictionary learning. We can extend the dictionary learning scheme readily to shape learning to achieve better results.

To eliminate the influence of different training datasets, We follow the setting (Omran et al. 2018) and train our model only on the Human3.6M dataset. We do not use any





Figure 3: Qualitative results on challenging 2D images from the LSP (Johnson and Everingham 2010), Human3.6M (Ionescu et al. 2014), and MPI-INF-3DHP (Mehta et al. 2017a) datasets.

Method	Surface Error
Lassner <i>et al.</i> (Lassner et al. 2017)	169.8
Pavlakos <i>et al.</i> (Pavlakos et al. 2018)	117.7
Ours (semi-supervised)	<b>110.1</b>

Table 3: UP-3D Results. UP-3D evaluates the shape error as mesh. Our favorable results show that the proposed dictionaries well distill the shape knowledge to transfer to the in-the-wild datasets.

Method	Parts		Fg vs Bg		Run Time
	Acc	F1	Acc	F1	
SMPLify from 91 kps (Bogo et al. 2016)	88.82	0.67	92.17	0.88	-
SMPLify (Lassner et al. 2017)	87.71	0.64	91.89	0.88	~ 1 min
Decision Forests (Lassner et al. 2017)	82.32	0.51	86.60	0.80	0.13 sec
HMR (Kanazawa et al. 2018)	87.12	0.60	91.67	0.87	0.04 sec
Ours (semi-supervised)	88.69	0.66	91.36	0.86	<b>0.003 sec</b>

Table 4: LSP Results. Our method performs better than HMR, and comparably with optimization methods which use segmentation labels.

shape annotations during network training. Table 5 shows that equipped with the proposed kinematic dictionary, our method even performs better than the methods trained with shape annotations. Since we propose the shape dictionary together with the kinematic dictionary, we study their effectiveness in Table 6. We measure the surface error on UP-3D dataset. We can see kinematic dictionary is key to the performance. Adding shape dictionary can yield slightly better results.

In supplementary material, we also compare our choice of sparsemax with other options in dictionary learning. All in

Method	Training Data	P2↓
HMR <sup>1</sup> (Kanazawa et al. 2018)	Human3.6M + MPI-INF-3DHP + LSP + MPII + COCO	56.8
HMR <sup>2</sup> (Kanazawa et al. 2018)	Human3.6M	77.6
NBF (Omran et al. 2018)	Human3.6M	59.9
Ours(Semi)	Human3.6M	<b>54.5</b>

Table 5: Influence of training data. Trained only on the Human3.6M dataset. Using the same dataset, our method is still the best, even better than the methods that use much more training data.

Method	Shape D	Kinematic D	Surface Error↓	$\Delta$
Baseline			141.2	-
+ shape D	✓		141.0	-0.2
+ Kinematic D		✓	114.5	-26.7
+ Both	✓	✓	<b>110.1</b>	-31.1

Table 6: Ablation results of different dictionaries. With both the kinematic and shape dictionaries, our method achieves the best result.

all, sparsemax could encourage the dictionary to cover the data better and improve the performance of pose estimation.

## Conclusion

In this paper, we propose a novel prior, the kinematic dictionary, to constrain the kinematic rotations of the human joints. We embed the kinematic dictionary into the deep learning framework. To make the dictionary learning consistent with the utilization of the dictionary in the network, we propose a novel objective function and introduce the sparse-

max into the learning algorithm. Our method achieves competitive results against the state-of-the-art on relevant benchmarks.

## References

- Akhter, I.; and Black, M. J. 2015. Pose-conditioned joint angle limits for 3D human pose reconstruction. In *Proceedings of the IEEE Conference on Computer Vision and Pattern Recognition*.
- Andriluka, M.; Pishchulin, L.; Gehler, P.; and Schiele, B. 2014. 2d human pose estimation: New benchmark and state of the art analysis. In *Proceedings of the IEEE Conference on Computer Vision and Pattern Recognition*.
- Anguelov, D.; Srinivasan, P.; Koller, D.; Thrun, S.; Rodgers, J.; and Davis, J. 2005. SCAPE: shape completion and animation of people. In *ACM SIGGRAPH 2005 Papers*, 408–416.
- Bogo, F.; Kanazawa, A.; Lassner, C.; Gehler, P.; Romero, J.; and Black, M. J. 2016. Keep it SMPL: Automatic estimation of 3D human pose and shape from a single image. In *European Conference on Computer Vision*. Springer.
- Cao, Z.; Simon, T.; Wei, S.-E.; and Sheikh, Y. 2017. Real-time Multi-Person 2D Pose Estimation Using Part Affinity Fields. In *The IEEE Conference on Computer Vision and Pattern Recognition*.
- Carfora, M. F. 2007. Interpolation on spherical geodesic grids: a comparative study. *Journal of Computational and Applied Mathematics* 210(1-2): 99–105.
- Chen, C.-H.; and Ramanan, D. 2017. 3d human pose estimation= 2d pose estimation+ matching. In *Proceedings of the IEEE Conference on Computer Vision and Pattern Recognition*.
- Dong, J.; Shuai, Q.; Zhang, Y.; Liu, X.; Zhou, X.; and Bao, H. 2020. Motion Capture from Internet Videos. *arXiv preprint arXiv:2008.07931*.
- Guler, R. A.; and Kokkinos, I. 2019. HoloPose: Holistic 3D Human Reconstruction In-The-Wild. In *The IEEE Conference on Computer Vision and Pattern Recognition*.
- Güler, R. A.; Neverova, N.; and Kokkinos, I. 2018. Densepose: Dense human pose estimation in the wild. In *Proceedings of the IEEE conference on computer vision and pattern recognition*.
- He, K.; Zhang, X.; Ren, S.; and Sun, J. 2016. Deep residual learning for image recognition. In *Proceedings of the IEEE Conference on Computer Vision and Pattern Recognition*.
- Ionescu, C.; Papava, D.; Olaru, V.; and Sminchisescu, C. 2014. Human3.6M: Large Scale Datasets and Predictive Methods for 3D Human Sensing in Natural Environments. *IEEE Transactions on Pattern Analysis and Machine Intelligence* 36(7): 1325–1339.
- Johnson, S.; and Everingham, M. 2010. Clustered Pose and Nonlinear Appearance Models for Human Pose Estimation. In *bmvc*.
- Joo, H.; Liu, H.; Tan, L.; Gui, L.; Nabbe, B.; Matthews, I.; Kanade, T.; Nobuhara, S.; and Sheikh, Y. 2015. Panoptic Studio: A Massively Multiview System for Social Motion Capture. In *The IEEE International Conference on Computer Vision*.
- Joo, H.; Simon, T.; Li, X.; Liu, H.; Tan, L.; Gui, L.; Banerjee, S.; Godisart, T. S.; Nabbe, B.; Matthews, I.; Kanade, T.; Nobuhara, S.; and Sheikh, Y. 2017. Panoptic Studio: A Massively Multiview System for Social Interaction Capture. *IEEE Transactions on Pattern Analysis and Machine Intelligence*.
- Kanazawa, A.; Black, M. J.; Jacobs, D. W.; and Malik, J. 2018. End-to-end recovery of human shape and pose. In *Proceedings of the IEEE Conference on Computer Vision and Pattern Recognition*.
- Kanazawa, A.; Zhang, J. Y.; Felsen, P.; and Malik, J. 2019. Learning 3d human dynamics from video. In *Proceedings of the IEEE Conference on Computer Vision and Pattern Recognition*.
- Kolotouros, N.; Pavlakos, G.; Black, M. J.; and Daniilidis, K. 2019. Learning to Reconstruct 3D Human Pose and Shape via Model-fitting in the Loop. In *Proceedings of the IEEE International Conference on Computer Vision*.
- Kolotouros, N.; Pavlakos, G.; and Daniilidis, K. 2019. Convolutional Mesh Regression for Single-Image Human Shape Reconstruction. In *Proceedings of the IEEE Conference on Computer Vision and Pattern Recognition*.
- Lassner, C.; Romero, J.; Kiefel, M.; Bogo, F.; Black, M. J.; and Gehler, P. V. 2017. Unite the people: Closing the loop between 3d and 2d human representations. In *Proceedings of the IEEE Conference on Computer Vision and Pattern Recognition*.
- Lin, T.-Y.; Maire, M.; Belongie, S.; Hays, J.; Perona, P.; Ramanan, D.; Dollár, P.; and Zitnick, C. L. 2014. Microsoft coco: Common objects in context. In *European Conference on Computer Vision*. Springer.
- Loper, M.; Mahmood, N.; and Black, M. J. 2014. MoSh: Motion and shape capture from sparse markers. *ACM Transactions on Graphics* 33(6): 220.
- Loper, M.; Mahmood, N.; Romero, J.; Pons-Moll, G.; and Black, M. J. 2015. SMPL: A skinned multi-person linear model. *ACM transactions on graphics* 34(6): 248.
- Luvizon, D. C.; Picard, D.; and Tabia, H. 2018. 2d/3d pose estimation and action recognition using multitask deep learning. In *Proceedings of the IEEE Conference on Computer Vision and Pattern Recognition*.
- Mairal, J.; Bach, F.; Ponce, J.; and Sapiro, G. 2009. Online dictionary learning for sparse coding. In *Proceedings of the 26th Annual International Conference on Machine Learning*. ACM.
- Martinez, J.; Hossain, R.; Romero, J.; and Little, J. J. 2017. A simple yet effective baseline for 3d human pose estimation. In *Proceedings of the IEEE International Conference on Computer Vision*.



- Martins, A.; and Astudillo, R. 2016. From softmax to sparsemax: A sparse model of attention and multi-label classification. In *International Conference on Machine Learning*.
- Mehta, D.; Rhodin, H.; Casas, D.; Fua, P.; Sotnychenko, O.; Xu, W.; and Theobalt, C. 2017a. Monocular 3d human pose estimation in the wild using improved cnn supervision. In *2017 international conference on 3D vision (3DV)*. IEEE.
- Mehta, D.; Sridhar, S.; Sotnychenko, O.; Rhodin, H.; Shafiei, M.; Seidel, H.-P.; Xu, W.; Casas, D.; and Theobalt, C. 2017b. Vnect: Real-time 3d human pose estimation with a single rgb camera. *ACM Transactions on Graphics* 36(4): 44.
- Moreno-Noguer, F. 2017. 3d human pose estimation from a single image via distance matrix regression. In *Proceedings of the IEEE Conference on Computer Vision and Pattern Recognition*.
- Newell, A.; Yang, K.; and Deng, J. 2016. Stacked hourglass networks for human pose estimation. In *European Conference on Computer Vision*. Springer.
- Nie, B. X.; Wei, P.; and Zhu, S.-C. 2017. Monocular 3d human pose estimation by predicting depth on joints. In *2017 IEEE International Conference on Computer Vision*. IEEE.
- Olshausen, B. A.; and Field, D. J. 1997. Sparse coding with an overcomplete basis set: A strategy employed by V1? *Vision research* 37(23): 3311–3325.
- Omran, M.; Lassner, C.; Pons-Moll, G.; Gehler, P.; and Schiele, B. 2018. Neural body fitting: Unifying deep learning and model based human pose and shape estimation. In *2018 International Conference on 3D Vision*. IEEE.
- Pavlakos, G.; Choutas, V.; Ghorbani, N.; Bolkart, T.; Osman, A. A. A.; Tzionas, D.; and Black, M. J. 2019. Expressive Body Capture: 3D Hands, Face, and Body from a Single Image. In *Proceedings IEEE Conf. on Computer Vision and Pattern Recognition (CVPR)*.
- Pavlakos, G.; Zhou, X.; Derpanis, K. G.; and Daniilidis, K. 2017. Coarse-to-fine volumetric prediction for single-image 3D human pose. In *Proceedings of the IEEE Conference on Computer Vision and Pattern Recognition*.
- Pavlakos, G.; Zhu, L.; Zhou, X.; and Daniilidis, K. 2018. Learning to estimate 3D human pose and shape from a single color image. In *Proceedings of the IEEE Conference on Computer Vision and Pattern Recognition*.
- Ramakrishna, V.; Kanade, T.; and Sheikh, Y. 2012. Reconstructing 3d human pose from 2d image landmarks. In *European Conference on Computer Vision*. Springer.
- Rogez, G.; and Schmid, C. 2016. Mocap-guided data augmentation for 3d pose estimation in the wild. In *Advances in neural information processing systems*.
- Romero, J.; Tzionas, D.; and Black, M. J. 2017. Embodied Hands: Modeling and Capturing Hands and Bodies Together. *ACM Transactions on Graphics, (Proc. SIGGRAPH Asia)* 36(6).
- Saini, N.; Price, E.; Tallamraju, R.; Enficiaud, R.; Ludwig, R.; Martinovic, I.; Ahmad, A.; and Black, M. J. 2019. Markerless Outdoor Human Motion Capture Using Multiple Autonomous Micro Aerial Vehicles. In *The IEEE International Conference on Computer Vision*.
- Shoemake, K. 1985. Animating rotation with quaternion curves. In *ACM SIGGRAPH computer graphics*. ACM.
- Sun, X.; Shang, J.; Liang, S.; and Wei, Y. 2017. Compositional human pose regression. In *Proceedings of the IEEE International Conference on Computer Vision*.
- Sun, X.; Xiao, B.; Wei, F.; Liang, S.; and Wei, Y. 2018. Integral human pose regression. In *Proceedings of the European Conference on Computer Vision*.
- Tan, V.; Budvytis, I.; and Cipolla, R. 2018. Indirect deep structured learning for 3d human body shape and pose prediction .
- Toshev, A.; and Szegedy, C. 2014. Deeppose: Human pose estimation via deep neural networks. In *Proceedings of the IEEE Conference on Computer Vision and Pattern Recognition*.
- Varol, G.; Ceylan, D.; Russell, B.; Yang, J.; Yumer, E.; Laptev, I.; and Schmid, C. 2018. Bodynet: Volumetric inference of 3d human body shapes. In *Proceedings of the European Conference on Computer Vision*.
- Wang, C.; Wang, Y.; Lin, Z.; Yuille, A. L.; and Gao, W. 2014. Robust estimation of 3d human poses from a single image. In *Proceedings of the IEEE Conference on Computer Vision and Pattern Recognition*.
- Wangni, J.; Lin, D.; Liu, J.; Daniilidis, K.; and Shi, J. 2018. Monocular 3D Pose Recovery via Nonconvex Sparsity with Theoretical Analysis. *arXiv preprint arXiv:1812.11295* .
- Wei, S.-E.; Ramakrishna, V.; Kanade, T.; and Sheikh, Y. 2016. Convolutional pose machines. In *Proceedings of the IEEE Conference on Computer Vision and Pattern Recognition*.
- Zhao, L.; Peng, X.; Tian, Y.; Kapadia, M.; and Metaxas, D. N. 2019. Semantic graph convolutional networks for 3d human pose regression. In *Proceedings of the IEEE/CVF Conference on Computer Vision and Pattern Recognition*.
- Zhou, X.; Huang, Q.; Sun, X.; Xue, X.; and Wei, Y. 2017. Towards 3d human pose estimation in the wild: a weakly-supervised approach. In *Proceedings of the IEEE International Conference on Computer Vision*.
- Zhou, X.; Leonardos, S.; Hu, X.; and Daniilidis, K. 2015. 3D shape estimation from 2D landmarks: A convex relaxation approach. In *proceedings of the IEEE Conference on Computer Vision and Pattern Recognition*.
- Zhou, X.; Sun, X.; Zhang, W.; Liang, S.; and Wei, Y. 2016a. Deep kinematic pose regression. In *European Conference on Computer Vision*. Springer.
- Zhou, X.; Zhu, M.; Leonardos, S.; Derpanis, K. G.; and Daniilidis, K. 2016b. Sparseness meets deepness: 3D human pose estimation from monocular video. In *Proceedings of the IEEE Conference on Computer Vision and Pattern Recognition*.

Zhou, Y.; Barnes, C.; Lu, J.; Yang, J.; and Li, H. 2019. On the continuity of rotation representations in neural networks. In *Proceedings of the IEEE Conference on Computer Vision and Pattern Recognition*.